13th World Conference on Earthquake Engineering
Vancouver, B.C., Canada
August 1-6, 2004
Paper No. 57

CONDUCTING PERFORMANCE EVALUATION OF SEISMIC ISOLATED ELEVATED BRIDGES USING DABS

Ping ZHU [1], Masato ABE[2] and Yozo FUJINO[3]

SUMMARY

This paper evaluates seismic performance of elevated bridges considering pounding between bridge girders/decks and pounding countermeasures. A general-purpose dynamic analysis program for bridges - DABS (Dynamic Analysis of Bridge Systems) has been implemented using detailed 3d modeling of an entire bridge including a 3D pounding model developed by the authors. Using DABS, a steel elevated bridge is modeled for a case study of performance evaluation by monitoring responses of girders, peak and residual gaps between girders and damage status of rubber bearing supporters.

INTRODUCTION

Elevated bridges play an important role in transportation of modern societies. During severe earthquakes, in addition to damage caused directly to bridge structures, a bridge may lose its functionality from the viewpoint of serviceability, even though the bridge itself has not collapsed. During the 1995 Kobe earthquake, the traffic service system in the emergency situation experienced substantial difficulties as considerable damage happened in elevated bridges. Impact damage to the ends of girders and the failure of bearings resulted in large gaps and/or unevenness between girders and a number of bridges were closed as a result. After the Kobe earthquake, the number of base-isolated bridges has increased tremendously. This needs proper treatment of pounding together with a total bridge structure because of large seismic-induced displacements of girders.

To meet this need, DABS has been developed based on 3D modeling of an entire bridge structure and arbitrary pounding between bridge girders. The first part of this paper presents 3D modeling of elevated bridges highlighting models of 3D pounding and rubber bearing. Implementations of DABS are introduced in the second part. A case study with a three-span steel bridge is presented in the final part.

---

[1] Ph.D. Research Institute of Science and Technology for Society, Japan Science and Technology Agency, Tokyo, Japan. Email:zhu@ristex.jst.go.jp
[2] Associate Professor, Dept. of Civil Engineering, University of Tokyo, Tokyo, Japan. Email:masato@bridge.t.u-tokyo.ac.jp
[3] Professor, Dept. of Civil Engineering, University of Tokyo, Tokyo, Japan. Email:fujino@bridge.t.u-tokyo.ac.jp

3D DETAILED MODELING OF ELEVATED BRIDGES

Elevated bridges are generally composed of foundations, piers, abutments, girders/decks, bearing supports and expansion joints. In addition, restrainers and bumpers are considered as pound mitigation devices. This section describes modeling of pounding, pounding mitigation devices and rubber bearings. Modeling of other components of an entire bridge is also presented.

Modeling of pounding between girders/decks

Considering the problem of arbitrary of two girders (Figure 1), a 3D contact-friction model was developed by Zhu et al [1]~[3]. This model is based on point-surface contact with penetration (Figure 2). The target surface, named as *abcd*, is assumed as a rigid plane. Node k is the contactor node at the contactor body, which penetrates into the target surface during contact. Point p is the physical contact point at the target surface *abcd*.

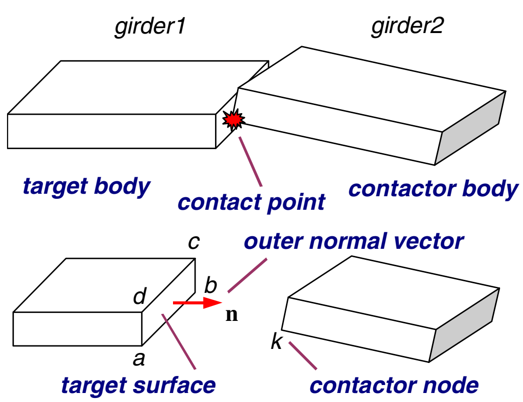

Fig. 1 Bridge girders in arbitrary contact.

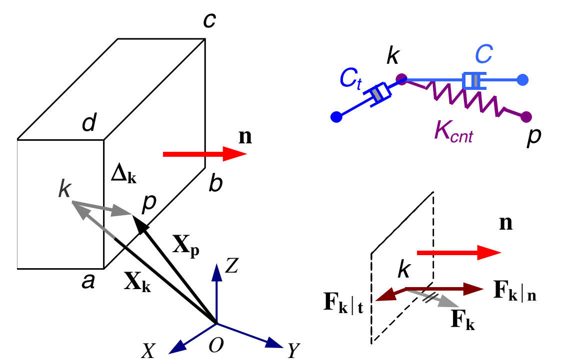

Fig. 2 Illustration of the 3D contact-friction model.

Upon contact, a universal spring K_{cnt} between node k and point p is created to compute the force of contact. Two dashpots, C and C_t, are also applied to node k for simulating energy loss during contact. The contact force at node k, $\mathbf{F_k}$, can be computed as:

$$\mathbf{F_k} = K_{cnt} \cdot \mathbf{\Delta_k} \tag{1}$$

$\mathbf{F_k}$ can be divided into normal and tangent components ($\mathbf{F_k|_n}$ and $\mathbf{F_k|_t}$ respectively), where vector $\mathbf{n}$ is the outer normal vector of the target surface and vector $\mathbf{t}$ is a projection vector of $\mathbf{F_k}$ to the target surface. During contact, status can be divided into stick contact and slide contact which can be decided by the ratio of tangent component of the contact force $|\mathbf{F_k|_t}|$ to the normal one $|\mathbf{F_k|_n}|$.

Contact status can be divided into stick and slide contact, which can be decided into stick and slide according to Equations 2a and 2b respectively.

$$\left|\mathbf{F_k}|_\mathbf{t}\right| < \mu_s \left|\mathbf{F_k}|_\mathbf{n}\right| \tag{2a}$$

$$\left|\mathbf{F_k}|_\mathbf{t}\right| \geq \mu_s \left|\mathbf{F_k}|_\mathbf{n}\right| \tag{2b}$$

where $\mathbf{F_k|_n}$, $\mathbf{F_k|_t}$ are normal and tangent components of $\mathbf{F_k}$ to the target surface respectively; and μ_s is static friction coefficient.

The contact force at the contactor node k can be calculated separately for stick and slide conditions, as given in Equations 3a and 3b respectively.

$$\mathbf{R_k} = \mathbf{F_k} + \mathbf{F_c}\big|_{\mathbf{n}} + \mathbf{F_c}\big|_{\mathbf{t}} \tag{3a}$$

$$\mathbf{R_k} = \mathbf{F_k}\big|_{\mathbf{n}} + \mathbf{F_c}\big|_{\mathbf{n}} + \mathbf{F_f}\big|_{\mathbf{t}} \tag{3b}$$

Components of damping forces at the normal and the tangent directions, $\mathbf{F_c}|_\mathbf{n}$ and $\mathbf{F_c}|_\mathbf{t}$, are given by Equations 3c and 3d respectively. Kinetic friction $\mathbf{F_f}|_\mathbf{t}$ is given by Equation 3e.

$$\mathbf{F_c}\big|_{\mathbf{n}} = -C \cdot \mathbf{V_{kp}}\big|_{\mathbf{n}} \tag{3c}$$

$$\mathbf{F_c}\big|_{\mathbf{t}} = -C_t \cdot \mathbf{V_{kp}}\big|_{\mathbf{t}} \tag{3d}$$

$$\mathbf{F_f}\big|_{\mathbf{t}} = -\mu_k \cdot \left|\mathbf{F_k}\big|_{\mathbf{n}}\right| \frac{\mathbf{V_{kp}}\big|_{\mathbf{t}}}{\left|\mathbf{V_{kp}}\big|_{\mathbf{t}}\right|} \tag{3e}$$

where $\mathbf{V_{kp}}$ is the relative velocity of node k to point p; and μ_k is kinetic friction coefficient.

Parameters of the model are chosen as follow:

The axial stiffness of the contactor body can be used as the stiffness of the universal spring K_{cnt}. As presented in Equation 4a. Damping ratios, C and C_t, can be determined according to the restitution coefficient at normal and tangent directions by Equations 4b and 4c.

$$K_{cnt} = \frac{EA}{L} \tag{4a}$$

$$C = 2\xi\sqrt{K_{cnt}\frac{M_1 M_2}{M_1 + M_2}} \tag{4b}$$

$$\xi = \frac{-\ln e}{\sqrt{\pi^2 + (\ln e)^2}} \tag{4c}$$

where E, A and L are modulus of elasticity, cross section area and length of the contactor element respectively; M_1 and M_2 are masses of the two bodies in contact; e is the restitution coefficient in the normal and the tangent directions (e and e_t, respectively); ξ is the damping ratio corresponding to restitution coefficient e.

Contact forces at the target surface can by obtained by linear interpolation according to static equilibrium. The total contact forces for a contact-pair are given in Equation 5.

$$\mathbf{R}_{\mathrm{cnt}}\big|_{cnt\_pair} = \begin{Bmatrix} \mathbf{R_k} \\ \mathbf{R}_{\mathrm{target\_surface}} \end{Bmatrix} = \begin{Bmatrix} \mathbf{R_k} \\ \mathbf{R_a} \\ \mathbf{R_b} \\ \mathbf{R_c} \\ \mathbf{R_d} \end{Bmatrix} \tag{5}$$

To simulate arbitrary pounding between two girders, contactor nodes and target surfaces are designated in both girders. As shown in Figure 3, contact pairs for *girder1* to *girder2*, which means nodes at *girder1* contact with target face on *girder2*, can be defined as (n_{1a}, *surface2*), (n_{1b}, *surface2*) etc. The same way is for contact pairs of *girder2* to *girder1*, which as (n_{2a}, *surface1*), (n_{2b}, *surface1*) etc. This is for the simplest case of contact between two girders. In fact, a node may be involved into more than one contact pairs (for instance, during to refined modeling of girder's ends), which means the node may contact with more than one surfaces, in most cases, not simultaneously, according to real situations.

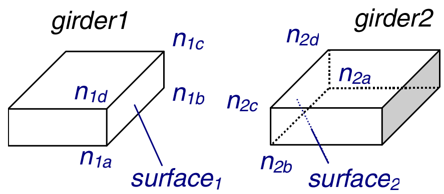

Fig. 3 An illustration of pounding modeling between two girders.

Restrainers and bumpers

Restrainers and bumpers are modeled in bilinear. As shown in Figure 4, a restrainer works in tension side as a linear spring with stiffness k_{0r} after an initial clearance d_{0r}. Similarly, a bumper works in compression side with stiffness k_{0b} after an initial clearance d_{0b}.

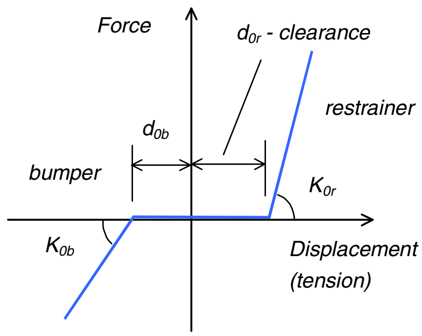

Fig. 4 Modeling of restrainers and bumpers.

Bi-axial model of rubber bearings

A biaxial model for rubber bearing by Yoshida et al (1999) [4], which is capable at two horizontal directions, is used in the analysis (Figure 5). The model is given by Equations 6a to 6g.

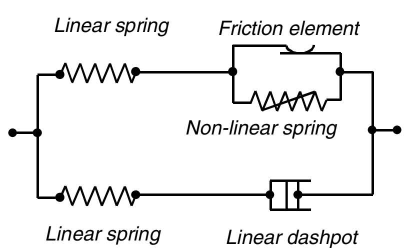

Fig. 5 Modeling of rubber bearings.

$$F_i = F_{i1} + F_{i2} \tag{6a}$$

$$\frac{\dot{F}_{i1}}{Y} = \frac{\dot{U}_i}{U_0} - \frac{\sqrt{\dot{U}_x^{\,2} + \dot{U}_y^{\,2}}}{U_0} \left| \frac{\sqrt{(F_{x1} - S_x)^2 + (F_{y1} - S_y)^2}}{Y} \right|^{n-1} \frac{F_{i1} - S_i}{Y} \tag{6b}$$

$$F_{i2} = \eta \dot{U}_i^{dashpot} = k U_i^{spring} \tag{6c}$$

$$U_i^{dashpot} + U_i^{spring} = U_i \tag{6d}$$

$$\frac{S_i}{Y} = \left(\frac{U_i}{U_0} - \frac{F_i}{Y}\right)\left(\alpha_0 - \beta\left|\frac{U_{\max}}{U_0}\right|^q\right) \tag{6e}$$

$$Y = Y_0\left\{1 + \gamma\left(\frac{\sqrt{U_x{}^2 + U_y{}^2}}{U_0}\right)^p\right\} \tag{6f}$$

$$U_{\max} = \sqrt{U_x{}^2 + U_y{}^2}\Big|_{\max\_past} \tag{6g}$$

where F_i, U_i, S_i are force, displacement and back force at i direction; Y, U_0 are yield load and displacement; α, β, γ, n, p, q, η are parameters; and $i=x,y$.

Modeling of other components [5]

The fiber model, known as a discretized-section model for nonlinear analysis (Li & Kubo 1998 [6], Zhu 2002 [5]), is used to model piers. A linear elastic straight beam element (Bathe 1996 [7]) is adopted for girders. Soil-structure interactions should also be taken into account. A soil-grouped pile model with simplifications has been adopted (Konagai 1999 [8]).

Governing equation

The governing equation of motion is given in Equation 7. To simulate pounding between girders, a vector of contact forces, $\mathbf{R_{cnt}}$, is added into the equation.

$$\mathbf{M_{ii}\ddot{u}_i} + \mathbf{C_{ii}\dot{u}_i} + \mathbf{K_{ii}u_i} = \mathbf{R_i} - \mathbf{M_{ib}\ddot{u}_b} - \mathbf{C_{ib}\dot{u}_b} - \mathbf{K_{ib}u_b} + \mathbf{R_{cnt}} \tag{7}$$

where i and b represent inner and boundary nodes respectively.

IMPLEMENTATION OF ANALYSIS PROGRAM – DABS

A general-purpose dynamic analysis program for bridges, DABS (Dynamic Analysis of Bridge Systems), has been developed by Zhu et al [1], [5]. DABS implements 3D models of bridge structures presented in this paper. Written in C++, DABS takes advantages of object-oriented programming to realize numerical models for bridge structures. A free-formatted text file input interface has been designed to model bridge structures and to give computing and output conditions. Crosschecks and tests of non-linear models of DABS were conducted [5]. A Web-based graphical post-processor for viewing seismic response of bridges was also developed [9].

PERFORMANCE EVALUATION USING A MODEL BRIDGE – A CASE STUDY

A typical three-span steel bridge has been selected for a case study. As shown in Figure 6, fiber model is adopted at the first segment of each pier from foundation. Base-isolation rubber bearings are applied for each pier. For computation of pounding, a simple supported girder in each span is assumed. Restrainers and bumpers are adopted as a countermeasure for pounding effect. Figure7 gives responses of the middle span under Takatori ground motion (1995 Kobe earthquake) with several cases.

Pounding between bridge girders, in addition to causing large reaction forces, may result in relative displacement between girders and may eventually cause unseating of the girders or generate significant vertical and horizontal gaps between the girders respectively. These residual gaps impede traffic, resulting in drastic decrease of rescue activities in the immediate aftermath of an earthquake disaster. In this study, this serviceability of elevated bridges is evaluated by estimate the magnitude of gaps between bridge girders. [10]

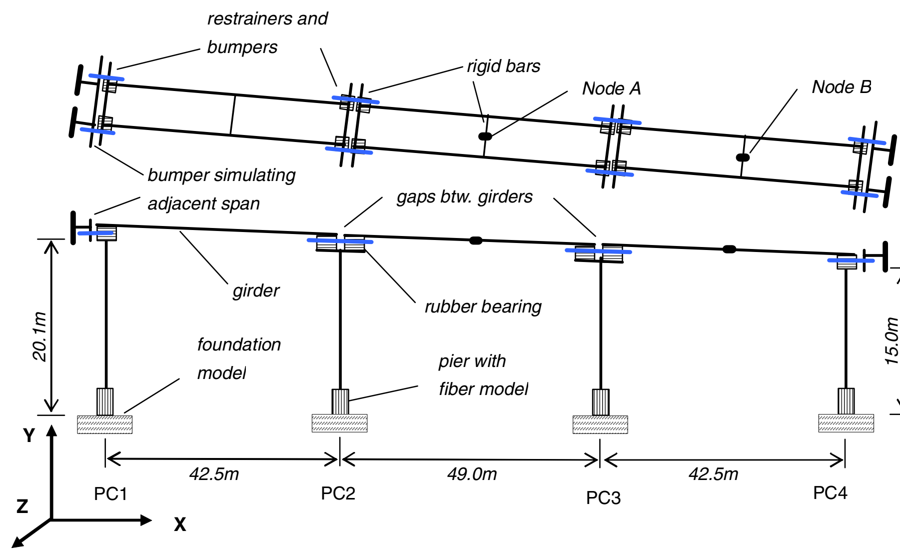

Fig. 6 Modeling of a three-span steel bridge.

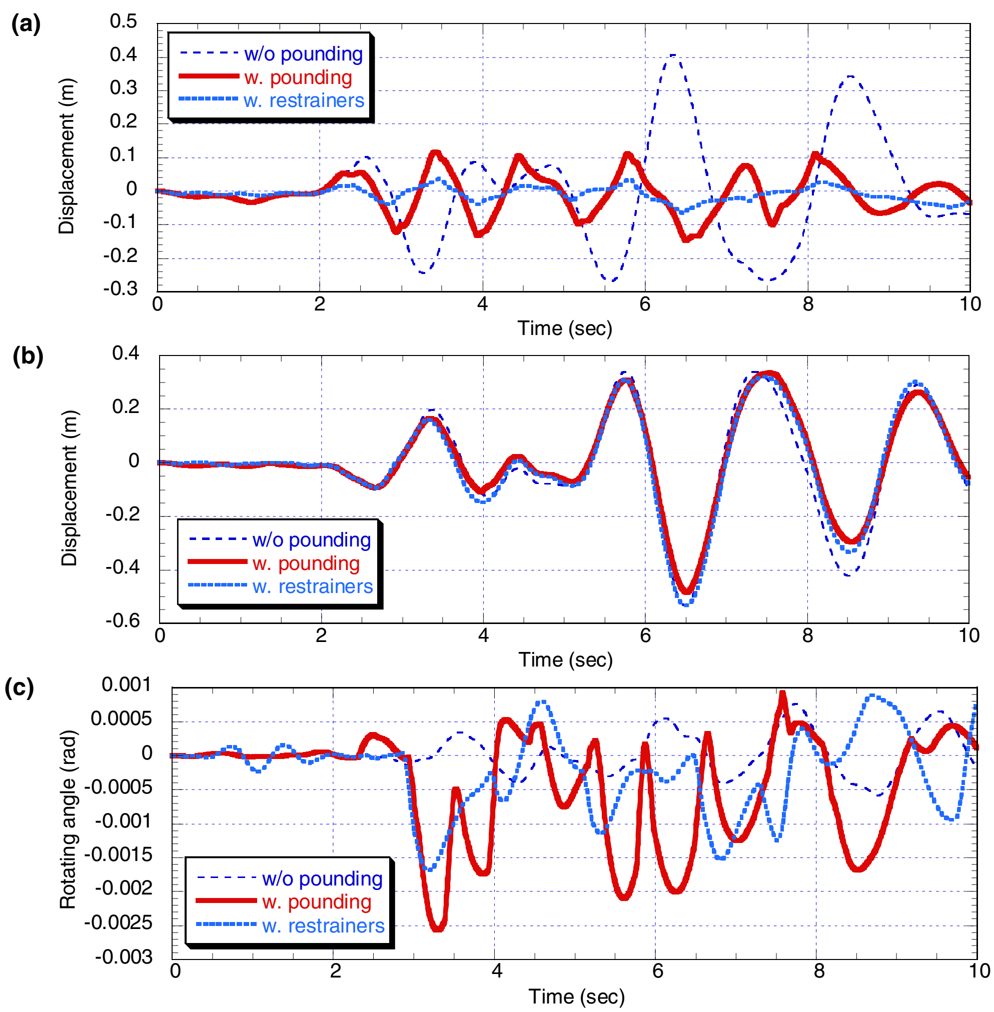

Fig. 7 Displacement comparisons of the mid span at node A: (a) Longitudinal, (b) Transversal, (c) Rotating.

To evaluate the serviceability of the three-span steel bridge, relative displacements between girders, denoted *Gap1* and *Gap2* (Figure 8), were observed. The relative displacements were measured between the center points at the ends of adjacent girders in the longitudinal and transversal directions. The relative displacements of the rubber bearings at the tops of piers *PC2* and *PC3* were also observed, where the rubber bearings are denoted *rbb20x* and *rbb30x* respectively. The time-history results of *Gap1* are given in Figure 9.

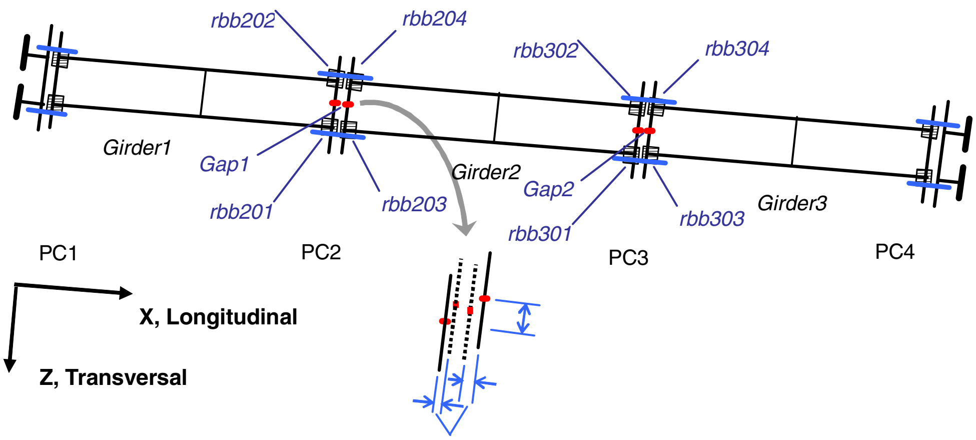

Fig. 8 Locations of serviceability evaluation of three-span steel bridge.

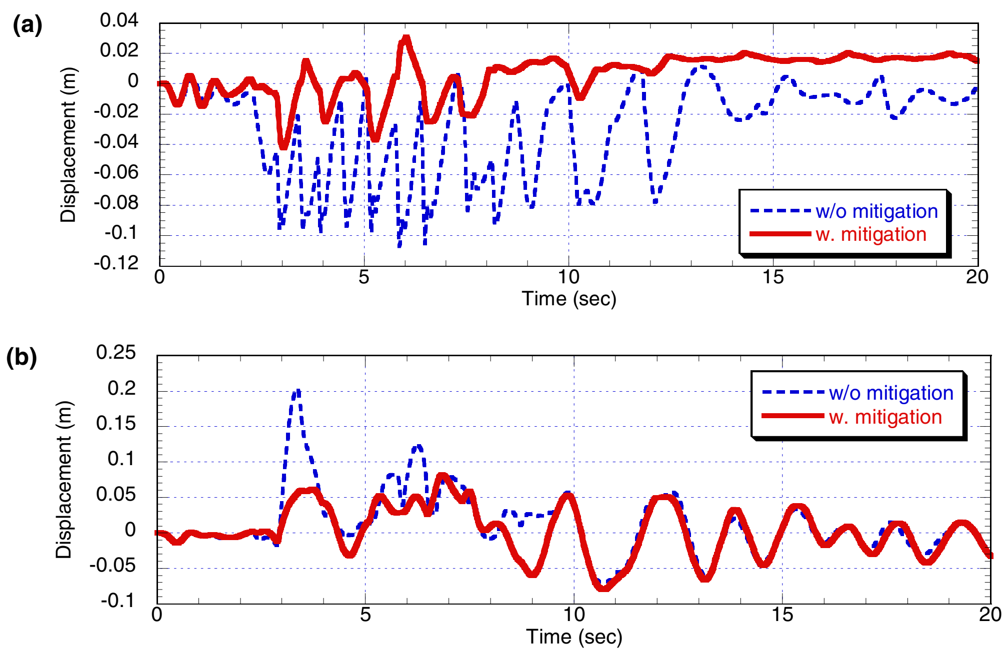

Fig. 9 Relative displacements between girders - Gap1:
(a) Longitudinal – Gap1x, (b) Transversal – Gap1z.

The failure of bearings is one of the primary causes of large vertical gaps between girders. According to the design specifications of highway bridges in Japan, the shear strain in the isolation bearing shall be within 250%. Experiments conducted by Uno et al (2000) [11] showed that the minimum shear strain of failure for rubber bearings can be 300%. Therefore, this study assumes a failure criterion for rubber bearings of a shear strain of 300%. Accordingly, damage to rubber bearings in both cases of without and with pounding mitigations is given in Figure 10.

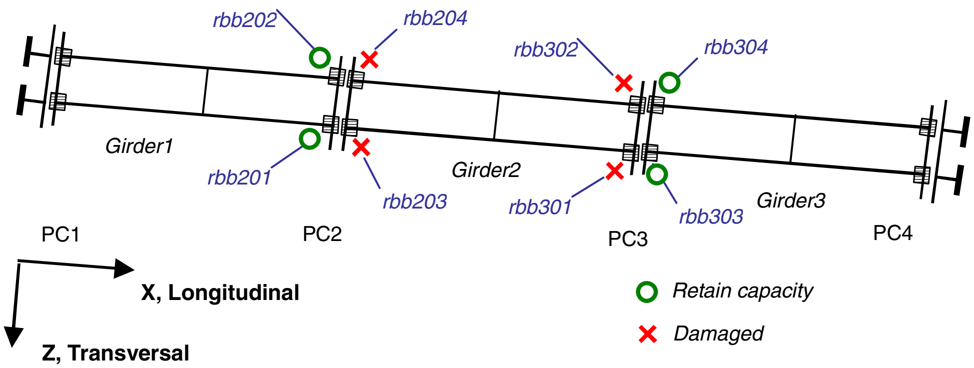

Fig. 10 Damage of rubber bearings.

CONCLUSIONS

This paper presented a practical way to establish detailed 3D modeling for elevated bridges including modeling of pounding between girders. Upon implementing a general-purpose dynamic analysis program - DABS, seismic performance of a model elevated bridge was conducted through a case study by monitoring the magnitude of maximum and residual gaps between girders in longitudinal and transversal directions and damage status of rubber bearing supporters.

From the case study, it can be observed that (1) pounding between girders can dramatically reduce the large seismic-induced displacement of bridge upper structures in the longitudinal direction caused by using rubber bearings (Figure 7), (2) the pounding countermeasure works in the longitudinal and the rotational directions (Figure 7), (3) maximum and residual gaps between girders in the longitudinal direction are not too large to harm the serviceability of the model bridge, (4) the pounding countermeasure works in reducing the maximum gap between girders in the transversal direction (Figure 9b), (5) failure of rubber bearing supporters occurs, this, in a consequence, may cause residual unevenness between girders and may harm the serviceability of the bridge.

REFERENCES

1. Zhu P. "Seismic Analysis and Serviceability Evaluation of Elevated Bridges on 3D Modeling with Pounding Effects of Girders". Ph. D. Dissertation, The University of Tokyo, 2001.
2. Zhu P, Abe M & Fujino Y. "A 3D Contact-friction Model for Pounding at Bridges during Earthquakes". Proceedings of The First M.I.T. Conference on Computational Fluid and Solid Mechanics, 2001, 575-578.
3 Zhu P, Abe M and Fujino Y. "Modeling Three Dimensional Non-linear Seismic Performance of Elevated Bridges with Emphasis on Pounding of Girders". Journal of Earthquake Engineering and Structural Dynamics 2002; 31: 1891-1913.
4 Yoshida J, Takesada S, Abe M & Fujino Y. "A bi-axial restoring force model on rubber bearings considering two-direction horizontal excitations" (in Japanese). Proceedings of the 25th Conference of Research on Earthquake Engineering 2: 741-744, 1999.
5 Zhu P, Abe M and Fujino Y. "A 3D General-Purpose Dynamic Analysis System for Bridges with Pounding Effects between Girders - Theory and Implementation", Third DIANA World Conference on Finite Elements in Civil Engineering Applications, Japan, 2002; 413-420.
6 Li KN & Kubo T. "Reviewing the multi-spring model and fiber model". The 10th Symposium on Earthquake Engineering of Japan: 2369-2374, 1998.

7 Bathe KJ. “Finite Element Procedures”. New Jersey: Prentice-Hall, Inc., 1996.

8 Konagai K. “Shaking table test allowing interpretation of damage to structure in terms of energy influx and efflux through soil-structure interface”. Report of Research Project 1999 Grant-in-aid for Scientific Research (B) (No. 10450174). The Ministry of Education, Science, Sports and Culture, Japan, 1999.

9 Zhu P, Abe M and Kiyono J. “A Graphical Post-processor for Web Oriented Applications”. Proceedings of JSCE Annual Conference, Japan, 2003.

10 Zhu P, Abe M and Fujino Y. “Evaluation of pounding countermeasures and serviceability of elevated bridges during seismic excitation using 3D modeling”. Journal of Earthquake Engineering and Structural Dynamics 2004; 33: 591-609.

11 Uno S, Morishige Y, Imai T and Takenouchi I. “Shearing Deformation Performance of Natural Rubber Bearings” (in Japanese). Proceedings of The Second Colloquium on Seismic Isolation and Response Control, Japan: 143-148, 2000.